SIMULATION OF SOUND ABSORPTION BY SCATTERING BODIES TREATED WITH ACOUSTIC LINERS USING A TIME-DOMAIN BOUNDARY ELEMENT METHOD

Michelle E. Rodio
Ph.D. Candidate, Department of Mathematics and Statistics
Old Dominion University, Norfolk, VA 23529, USA

Fang Q. Hu
Faculty Advisor, Department of Mathematics and Statistics
Old Dominion University, Norfolk, VA 23529, USA

Abstract

Reducing aircraft noise is a major objective in the field of computational aeroacoustics. When designing next generation quiet aircraft, it is important to be able to accurately and efficiently predict the acoustic scattering by an aircraft body from a given noise source. Acoustic liners are an effective tool for achieving aircraft noise reduction and are characterized by a frequency-dependent impedance (or admittance, defined as the inverse of impedance) value. Converted into the time-domain using Fourier transforms, an impedance boundary condition can be used to simulate the acoustic wave scattering by geometric bodies treated with acoustic liners. Two different acoustic liner models will be discussed in which the liner impedance is specified at a given frequency. Both impedance and admittance boundary conditions will be derived for each model and coupled with a time-domain boundary integral equation to model acoustic scattering by a flat plate consisting of both un-lined and lined surfaces. The scattering solution will be obtained iteratively using both spatial and temporal basis functions and the stability will be demonstrated through eigenvalue analysis.

Introduction

Reducing aircraft noise is a major objective in the field of computational aeroacoustics. When designing next generation quiet aircraft, it is important to be able to accurately and efficiently predict the acoustic scattering by an aircraft body from a given noise source [1] [2] [3] [4]. Acoustic scattering problems can be modeled using boundary element methods (BEMs) by reformulating the linear convective wave equation as a boundary integral equation (BIE), both in the frequency-domain and the time-domain; BEMs reduce the spatial dimension by one allowing for the integration over a surface instead of a volume [5] [6] [7] [8] [9] [10].

Frequency-domain solvers are the most commonly used and researched within literature; they have a reduced computational cost [11] and allow for modeling time-harmonic fields at a single frequency [10] [11] [12]. Moreover, frequency-domain solvers eliminate the growth of Kelvin-Helmholtz instabilities caused by the velocity shear of two interacting fluids, and allow for an impedance boundary condition to be imposed more naturally [12].

Despite the benefits of frequency-domain solvers, there are several distinct advantages to using time-domain solvers [1] [13]. For example, time-domain solvers allow for the simulation and study of broadband sources and time-dependent transient signals whereas studying broadband sources in the frequency-domain carry a high computational cost. Time-domain solvers also allow for the scattering solution at all frequencies to be obtained within a single computation and avoid needing to invert a large dense linear system as is required in the frequency-domain. Moreover, a time-domain solution is more naturally coupled with a nonlinear computational fluids dynamics simulation of noise sources.

Time-domain BIEs (TD-BIEs) unfortunately have an intrinsic numerical instability due to resonant frequencies, which result from non-trivial solutions in the interior domain. TD-BIE solvers also carry a high computational cost. In recent years, numerical techniques for modeling acoustic wave scattering using TD-BIEs have been under development [1] [2] [3] [4]. It has been shown that stability can be realized through implementing a Burton-Miller type reformulation of the TD-BIE and computational cost can be reduced using fast-algorithms and high performance computing.

In the present study, a time-domain BEM (TD-BEM) is used to solve a Burton-Miller type TD-BIE reformulated from the convective wave equation. The scattering solution is obtained using temporal and spatial basis functions and a March-On-in-Time scheme in which a sparse matrix is solved iteratively. Scattering problems are considered for geometric bodies consisting of both rigid and soft surfaces – surfaces in which an acoustic liner is applied. Typically composed of an array of Helmholtz resonators, acoustic liners are used for dissipating the incident acoustic wave and are

incredibly effective at absorbing sound in a specified frequency band [13] [14] [15].

Acoustic liners are characterized by a frequency-dependent impedance value, herein denoted by $Z(\omega)$. Impedance is a complex-valued quantity such that $\mathrm{Re}(Z)$ is given to be the acoustic resistance and $\mathrm{Im}(Z)$ is given to be the acoustic reactance [13] [14] [15]. Transformed into the time-domain using Fourier transforms, an impedance boundary condition may be coupled with a TD-BIE to model acoustic wave scattering by soft surfaces. Alternatively, an admittance boundary condition may also be used. Admittance, herein denoted by $Y(\omega)$, is defined to be the inverse of impedance: $Y(\omega) = 1/Z(\omega)$.

The present study will assess the numerical stability of the TD-BIE when modeling acoustic wave scattering by a flat plate consisting of soft surfaces, as a continuation from earlier work [16]. Both an impedance and admittance boundary condition will be studied. Moreover, two models will be considered when simulating the acoustic liner: an *Extended Helmholtz Resonator Model* [14] and a *Three-Parameter Impedance Model* [17]. In each model, the acoustic liner impedance is specified at a single frequency ω_0.

Derivation of the Time-Domain BIE

We aim to accurately and efficiently predict the scattering of a sound field by an object from a given noise source in the presence of a constant mean flow as shown in Figure 1. Acoustic waves are assumed to be disturbances of small amplitudes. With constant mean flow, the acoustic disturbances are governed by the linear convective wave equation [18], written as follows:

$$\left(\frac{\partial}{\partial t} + \boldsymbol{U}\cdot\boldsymbol{\nabla}\right)^2 p(\boldsymbol{r},t) - c^2\boldsymbol{\nabla}^2 p(\boldsymbol{r},t) = q(\boldsymbol{r},t) \qquad (1)$$

with homogeneous initial conditions:

$$p(\boldsymbol{r},0) = \frac{\partial p}{\partial t}(\boldsymbol{r},0) = 0, t = 0 \qquad (2)$$

where $p(\boldsymbol{r},t)$ is the acoustic pressure, $q(\boldsymbol{r},t)$ is the known acoustic source, and c is the speed of sound. Equations (1) and (2) are to be supplemented with suitable boundary conditions on the scattering surface. These conditions will be discussed in the subsequent section.

It is well known that the linear convective wave equation (1) and initial conditions (2), along with suitable boundary conditions, can be reformulated into an integral equation. As demonstrated in [16] and [19], the wave propagation problem can be reformulated into a TD-BIE by introducing a free-space adjoint Green's function $\tilde{G}$ with homogenous initial conditions $\tilde{G}(\boldsymbol{r},t;\boldsymbol{r}',t') = \partial\tilde{G}(\boldsymbol{r},t;\boldsymbol{r}',t')/\partial t = 0$ for $t > t'$. This reformulation yields the Kirchhoff integral representation of the acoustic field in the presence of a uniform mean flow $\boldsymbol{U}$:

$$\begin{aligned} p(\boldsymbol{r}',t') = &\int_{0-}^{t'+}\int_V \tilde{G}\, q(\boldsymbol{r},t)\, d\boldsymbol{r}dt \\ &+ c^2\int_{0-}^{t'+}\int_S \left(\tilde{G}\frac{\partial p}{\partial \bar{n}} - p\frac{\partial \tilde{G}}{\partial \bar{n}}\right) d\boldsymbol{r_s}dt \\ &- c\int_{0-}^{t'+}\int_S \left(\tilde{G}\frac{\partial p}{\partial t} - p\frac{\partial \tilde{G}}{\partial t}\right) M_n d\boldsymbol{r_s}dt \end{aligned} \qquad (3)$$

where $M = |\boldsymbol{M}|$ is the magnitude of the Mach number $\boldsymbol{M} = \boldsymbol{U}/c$, $\boldsymbol{r}'$ is an arbitrary point on the scattering body surface, $\partial/\partial\bar{n} = (\boldsymbol{n} - M_n\boldsymbol{M})\cdot\boldsymbol{\nabla}$, and $M_n = \boldsymbol{M}\cdot\boldsymbol{n}$ such that n is the inward normal vector on the scattering body S.

By letting $\partial/\partial\tilde{n} = \partial/\partial\bar{n} - (M_n/c)\partial/\partial t$, the TD-BIE results by expressing Eq. (3) in terms of retarded time values t_R' and taking the limit as $\boldsymbol{r}' \to \boldsymbol{r_s'}$ assuming $\boldsymbol{r_s'}$ is a smooth boundary collocation point. The resulting TD-BIE relates the solution p at point $\boldsymbol{r_s'}$ and time t' to the direct contribution from external sources $q(\boldsymbol{r},t_R')$ to the surface point $\boldsymbol{r_s'}$ and a contribution from both the source surface and scattering surface involving the retarded time values of p and their normal derivatives. A detailed derivation of the resulting TD-BIE is given in [16].

Derivation of the Liner Boundary Condition

For sound scattering problems, the solution $p(\boldsymbol{r_s'},t)$ on S is determined when the boundary condition for p on S is given. In this work, we assume that the scattering surface S consists of both rigid surfaces – denoted herein by S_0 – and soft surfaces – denoted herein by S_l, i.e., $S = S_0 \cup S_l$. On rigid surfaces, we impose the Zero Energy Flux boundary condition [19]:

$$\frac{\partial p}{\partial \tilde{n}}(\boldsymbol{r_s},t) = 0, \boldsymbol{r_s} \in S_0 \qquad (4)$$

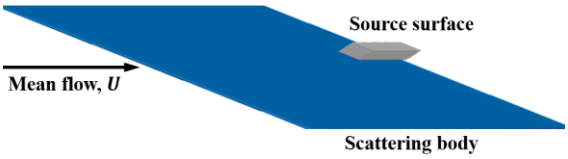

Figure 1: Schematic diagram illustrating the relationship between the mean flow, the surface of the scattering body, and the surface of the acoustic source.

On soft surfaces, $\partial p/\partial \tilde{n}$ is a non-zero term herein denoted by P_n, i.e.,

$$\frac{\partial p}{\partial \tilde{n}}(\boldsymbol{r_s}, t) = \begin{cases} P_n(\boldsymbol{r_s}, t) & \boldsymbol{r_s} \in S_l \\ 0 & \boldsymbol{r_s} \in S_0 \end{cases} \quad (5)$$

For simplicity, we assume $M_n = 0$ on soft surfaces; i.e., we assume that the mean flow is always tangent to the surface whereever the liner is installed. Under this assumption, $\partial p/\partial \tilde{n}$ is equal to $\partial p/\partial n$.

To derive a suitable boundary condition P_n, we consider a geometric body with soft surfaces and assume a model with no mean flow; i.e. Mach number $M = 0$. The acoustic pressure $p(\boldsymbol{r_s}, \omega)$ is given in the frequency-domain by:

$$p(\boldsymbol{r_s}, \omega) = Z(\omega) v(\boldsymbol{r_s}, \omega), \quad (6)$$

where $v(\boldsymbol{r_s}, \omega) = \boldsymbol{v} \cdot \boldsymbol{n}$, $\boldsymbol{v}$ is the acoustic velocity vector, $\boldsymbol{n}$ is the inward normal vector on the scattering body S, and $Z(\omega)$ is the surface impedance. Moreover, v can be represented by [9]:

$$v(\boldsymbol{r_s}, \omega) = \frac{1}{i\omega\rho_0} P_n(\boldsymbol{r_s}, \omega) \quad (7)$$

where $P_n(\boldsymbol{r_s}, \omega)$ is the normal derivative of acoustic pressure defined by Eq. (5), ρ_0 is the average fluid density, and i is the imaginary unit ($i^2 = -1$). Substituting (7) into (6) yields the following frequency-domain impedance boundary condition:

$$i\omega p(\boldsymbol{r_s}, \omega) = \frac{1}{\rho_0} Z(\omega) P_n(\boldsymbol{r_s}, \omega) \quad (8)$$

Using the inverse Fourier transform convolution property and causality condition which states $z(t-\tau) = 0$ for all $t - \tau > 0$, i.e., $z(t-\tau) = 0$ for all $t > \tau$, (8) can be transformed into the time-domain yielding a time-domain impedance boundary condition:

$$\rho_0 \frac{\partial p}{\partial t}(\boldsymbol{r_s}, t) = \frac{1}{2\pi} \int_{-\infty}^{t} z(t-\tau) P_n(\boldsymbol{r_s}, \tau) d\tau \quad (9)$$

Similarly, a time-domain admittance boundary condition is given by:

$$P_n(\boldsymbol{r_s}, t) = \frac{\rho_0}{2\pi} \int_{-\infty}^{t} \frac{\partial y}{\partial t}(t-\tau) p(\boldsymbol{r_s}, \tau) d\tau \quad (10)$$

Equations (9) and (10) establish two suitable boundary conditions for the TD-BIE necessary for modeling acoustic wave scattering by an object consisting of soft surfaces.

Derivation of the March-On-in-Time Scheme

The TD-BIE for solid wall boundary conditions has been known to have an intrinsic numerical instability due to resonant frequencies resulting from non-trivial solutions in the interior domain. Using a Burton-Miller type reformulation of the TD-BIE, resonant frequencies can be eliminated and stability achieved [1] [2] [3] [4]. The reformulation results from first taking the derivative of the TD-BIE in the form of $\tilde{a}$ multiplied by the time-derivative plus $\tilde{b}c$ multiplied by the normal derivative, where $\tilde{a}$ and $\tilde{b}$ define the stability condition, $\tilde{a}/\tilde{b} < 0$, and second taking the limit as $\boldsymbol{r'} \to \boldsymbol{r'_s}$. A detailed derivation of the resulting Burton-Miller type reformulation is given in [16].

The stable reformulation is discretized by dividing S into boundary elements using surface element basis functions $\phi_j(\boldsymbol{r_s})$ at node j and temporal basis functions $\psi_k(t)$ at time k:

$$p(\boldsymbol{r_s}, t) = \sum_{k=0}^{N_t} \sum_{j=1}^{N_e} u_j^k \phi_j(\boldsymbol{r_s}) \psi_k(t) \quad (11)$$

$$P_n(\boldsymbol{r_s}, t) = \sum_{k=0}^{N_t} \sum_{j=1}^{N_e} v_j^k \phi_j(\boldsymbol{r_s}) \psi_k(t) \quad (12)$$

where $v_j^k \equiv 0$ by default on any element E_j on rigid surfaces S_0. In Eqs. (11) and (12), N_e denotes the total number of surface nodes and N_t denotes the number of time-steps.

Let the spatial and temporal basis be defined as follows:

$$\phi_j(\boldsymbol{r_s}) = \begin{cases} 1 & \boldsymbol{r_s} \text{ on } E_j \text{ that contains node } r_j \\ 0 & \text{other} \end{cases} \quad (13)$$

$$\psi_k(t) = \Psi\left(\frac{t - t_k}{\Delta t}\right) \text{ such that:} \quad (14)$$

$$\Psi(\tau) = \begin{cases} 1 + 11\tau/6 + \tau^2 + \tau^3/6 & -1 < \tau \le 0 \\ 1 + \tau/2 - \tau^2 - \tau^3/2 & 0 < \tau \le 1 \\ 1 - \tau/2 - \tau^2 + \tau^3/2 & 1 < \tau \le 2 \\ 1 - 11\tau/6 + \tau^2 - \tau^3/6 & 2 < \tau \le 3 \end{cases} \quad (15)$$

and $\Psi(\tau) = 0$ for all other values of τ. By evaluating the discretized Burton-Miller type reformulation at collocation points $r_s = r_i$ and time-step $t' = t_n$, we obtain the following system of equations:

$$\begin{aligned}\boldsymbol{B_0 u^n + C_0 v^n} = \boldsymbol{q^n} &- \boldsymbol{B_1 u^{n-1}} - \boldsymbol{C_1 v^{n-1}} \\ &- \boldsymbol{B_2 u^{n-2}} - \boldsymbol{C_2 v^{n-2}} - \cdots \\ &- \boldsymbol{B_J u^{n-J}} - \boldsymbol{C_J v^{n-J}}\end{aligned} \quad (16)$$

where $\boldsymbol{u^k}$ and $\boldsymbol{v^k}$ denote the vector that contains all unknowns $\{u_j^k, j = 1, \dots, N_e\}$ and $\{v_j^k, j = 1, \dots, N_e\}$, respectively, at time level t_k. The non-zero entries for B and $\boldsymbol{C}$ are given in [16].

Recall that $v_j^k \equiv 0$ by default on any element E_j on rigid surfaces S_0. Assuming rigid body scattering only, $\boldsymbol{v^k}$ is equivalently equal to zero thereby reducing (16) to:

$$\boldsymbol{B_0 u^n} = \boldsymbol{q^n} - \boldsymbol{B_1 u^{n-1}} - \cdots - \boldsymbol{B_J u^{n-J}}, \quad (17)$$

the solution of which is easily obtained through an iterative process.

In the present study, we aim to demonstrate that stability can be achieved for scattering bodies with both rigid and soft surfaces. A second system of equations is therefore need to obtain solutions for both $\boldsymbol{u^k}$ and $\boldsymbol{v^k}$ and is derived by considering the discretization of either (9) or (10) at collocation point $\boldsymbol{r_s}$ and time-step t'. The resulting system can then be cast into the following matrix form with a finite number of K time steps:

$$\begin{aligned}\boldsymbol{D_0 u^n + E_0 v^n} = &-\boldsymbol{D_1 u^{n-1}} - \boldsymbol{E_1 v^{n-1}} \\ &-\boldsymbol{D_2 u^{n-2}} - \boldsymbol{E_2 v^{n-2}} - \cdots \\ &-\boldsymbol{D_K u^{n-K}} - \boldsymbol{E_K v^{n-K}}\end{aligned} \quad (18)$$

The non-zero entries for $\boldsymbol{D}$ and $\boldsymbol{E}$ are denoted by $\{\boldsymbol{D_k}\}_{ij}$ and $\{\boldsymbol{E_k}\}_{ij}$, respectively. The derivations for $\boldsymbol{D}$ and $\boldsymbol{E}$ are specific to the type of acoustic liner, simulated herein by either the *Extended Helmholtz Resonator Model* or *Three-Parameter Impedance Model*. These derivations will be discussed further in later sections.

Coupling (18) with (16) forms a March-On-in-Time scheme for the time-domain solution of the stable Burton-Miller type TD-BIE reformulation. The coupled system can be expressed as:

$$\begin{aligned}\begin{bmatrix}\boldsymbol{B_0} & \boldsymbol{C_0} \\ \boldsymbol{D_0} & \boldsymbol{E_0}\end{bmatrix}\begin{bmatrix}\boldsymbol{u^n} \\ \boldsymbol{v^n}\end{bmatrix} = \begin{bmatrix}\boldsymbol{q^n} \\ \boldsymbol{0}\end{bmatrix} &- \begin{bmatrix}\boldsymbol{B_1} & \boldsymbol{C_1} \\ \boldsymbol{D_1} & \boldsymbol{E_1}\end{bmatrix}\begin{bmatrix}\boldsymbol{u^{n-1}} \\ \boldsymbol{v^{n-1}}\end{bmatrix} \\ &- \begin{bmatrix}\boldsymbol{B_2} & \boldsymbol{C_2} \\ \boldsymbol{D_2} & \boldsymbol{E_2}\end{bmatrix}\begin{bmatrix}\boldsymbol{u^{n-2}} \\ \boldsymbol{v^{n-2}}\end{bmatrix} - \cdots - \\ &- \begin{bmatrix}\boldsymbol{B_K} & \boldsymbol{C_K} \\ \boldsymbol{D_K} & \boldsymbol{E_K}\end{bmatrix}\begin{bmatrix}\boldsymbol{u^{n-K}} \\ \boldsymbol{v^{n-K}}\end{bmatrix} - \cdots - \\ &- \begin{bmatrix}\boldsymbol{B_J} & \boldsymbol{0} \\ \boldsymbol{0} & \boldsymbol{0}\end{bmatrix}\begin{bmatrix}\boldsymbol{u^{n-J}} \\ \boldsymbol{v^{n-J}}\end{bmatrix}\end{aligned} \quad (19)$$

For locally reacting liners, the liner boundary condition is given pointwise. It follows that the coefficients in (19) are all diagonal matrices. In fact, if the liner impedance is the same on all soft boundaries, we have coefficient matrices in the form $\boldsymbol{D_k} = d_k \boldsymbol{I}$ and $\boldsymbol{E_k} = e_k \boldsymbol{I}$ where $k = 0,1, \dots, \boldsymbol{K}$, $\boldsymbol{I}$ is the identity matrix, and d_k, e_k are the coefficients for the time-domain liner boundary condition that is the same for all liner elements.

Extended Helmholtz Resonator Model

We first introduce the *Extended Helmholtz Resonator Model* to derive matrices $\boldsymbol{D}$ and $\boldsymbol{E}$ in (18). In this model, the frequency-domain surface impedance is defined to be:

$$Z(\omega) = F_R + i\omega m - iF_\beta \cot\left(\frac{1}{2}\omega\nu\Delta t - i\frac{1}{2}\epsilon\right) \quad (20)$$

where for an acoustic liner represented by a wall consisting of an array of Helmholtz resonators (Figure 2): F_R is the face-sheet resistance, ωm is the face-sheet mass reactance, $-\cot(\cdots)$ is the cavity reactance, F_β is a parameter used for varying the cavity reactance, Δt is the time-step, ϵ is the damping in the cavity's fluid, and $\nu\Delta t = 2L/c$ is a multiple of the time-step and proportional to two times the cavity length L divided by the speed of sound c.

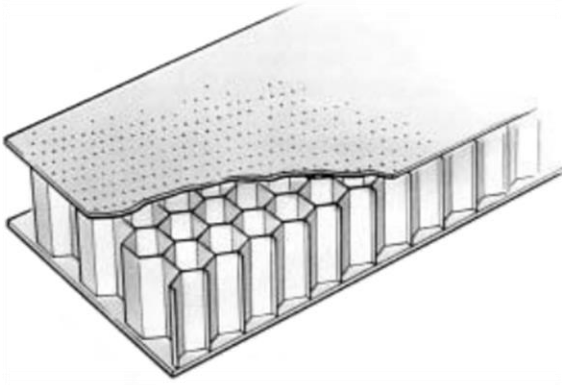

Figure 2: Acoustic liner diagram consisting of an array of Helmholtz Resonators.

In (20), $F_R, m, L, c, \epsilon \geq 0$. The model is both passive and casual [14]. For $\mathrm{Im}(\omega) < \epsilon/(\nu\Delta t)$, (20) becomes:

$$Z(\omega) = F_R + i\omega m + F_\beta + 2F_\beta \sum_{N=1}^{\infty} e^{-i\omega N\nu\Delta t - \epsilon N} \quad (21)$$

which, by taking the inverse Fourier transform, leads to a time-domain representation of surface impedance. In this model, the coefficients F_R and F_β

are specified at a given frequeny $\omega = \omega_0 > 0$. Moreover, letting the surface admittance be represented in the form $Z(\omega) = A + Bi$, we choose ϵ to be $\epsilon = 0.9\,\mathrm{arcsinh}(-(A/B)\sin(\omega_0 \nu \Delta t)) \geq 0$ following [14]. Substituting (21) into (9), we obtain an impedance boundary condition for soft surfaces. Casting into matrix form, the non-zero entries for $\boldsymbol{D}$ and $\boldsymbol{E}$ are, respectively:

$$\{\boldsymbol{D_k}\}_{ij} = \delta_{ij}\rho_0\psi'_{n-k}(t_n) \tag{22}$$

$$\{\boldsymbol{E_k}\}_{ij} = \delta_{ij}\left[\left(F_R + F_\beta\right)\psi_{n-k}(t_n) + m\psi'_{n-k}(t_n) + 2F_\beta \sum_{N=1}^{\infty} e^{-\epsilon N}\psi_{n-k}(t_n - N\nu\Delta t)\right] \tag{23}$$

where δ_{ij} is a Kronecker delta function and a prime denotes a derivative with respect to time.

Due to the limited temporal stencil width shown in Eqs. (13) through (15), the matrices $\boldsymbol{D}$ and $\boldsymbol{E}$ are sparse and represent interactions within the same element or nearby nodes at the same time level t_n. Moreover, the matrices are diagonally dominant and of the form $\boldsymbol{D_k} = d_k\boldsymbol{I}$ and $\boldsymbol{E_k} = e_k\boldsymbol{I}$ where $k = 0,1,\dots,\boldsymbol{K}$ and $\boldsymbol{I}$ is the identity matrix. In particular, the coefficients d_k and e_k simplify to:

$$d_k = \rho_0\begin{cases} 11/6 & k = 0 \\ -3 & k = 1 \\ 3/2 & k = 2 \\ -1/3 & k = 3 \\ 0 & \text{other} \end{cases} \tag{24}$$

$$e_k = \left(F_R + F_\beta\right)\begin{cases} 1 & k = 0 \\ 0 & k \neq 0 \end{cases} + m\begin{cases} 11/6 & k = 0 \\ -3 & k = 1 \\ 3/2 & k = 2 \\ -1/3 & k = 3 \\ 0 & \text{other} \end{cases}$$

$$+2F_\beta \textstyle\sum_{N=1}^{\infty} e^{-\epsilon N}\begin{cases} 1 & k - N\nu = 0 \\ 0 & k - N\nu \neq 0 \end{cases} \tag{25}$$

Similarly, we may assume the frequency-domain surface admittance model to be:

$$Y(\omega) = \overline{F_R} + i\omega m + \overline{F_\beta} + 2\overline{F_\beta}\sum_{N=1}^{\infty} e^{-i\omega N\nu\Delta t - \epsilon N} \tag{26}$$

Letting the surface admittance be represented in the form for $Y(\omega) = \overline{A} + \overline{B}i$, taking the inverse Fourier transform, and substituting into (10) yields an admittance boundary condition for soft surfaces, the details of which are outlined in [16]. Casting into matrix form, the non-zero entries for $\boldsymbol{D}$ and $\boldsymbol{E}$ have coefficients d_k and e_k which simplify to:

$$d_k = \rho_0\left(\overline{F_R} + \overline{F_\beta}\right)\begin{cases} 11/6 & k = 0 \\ -3 & k = 1 \\ 3/2 & k = 2 \\ -1/3 & k = 3 \\ 0 & \text{other} \end{cases}$$

$$-\rho_0 m\begin{cases} 2 & k = 0 \\ -5 & k = 1 \\ 4 & k = 2 \\ -1 & k = 3 \\ 0 & \text{other} \end{cases} \tag{27}$$

$$+2\rho_0 F_\beta \sum_{N=1}^{\infty} e^{-\epsilon N}\begin{cases} 11/6 & k = 0 \\ -3 & k = 1 \\ 3/2 & k = 2 \\ -1/3 & k = 3 \\ 0 & \text{other} \end{cases}$$

$$e_k = \begin{cases} 1 & k = 0 \\ 0 & k \neq 0 \end{cases} \tag{28}$$

Three-Parameter Impedance Model

We now introduce the *Three-Parameter Impedance Model* to derive matrices $\boldsymbol{D}$ and $\boldsymbol{E}$ in (18). In this model, the frequency-domain surface impedance is defined to be:

$$Z(\omega) = R_0 + h_0(-i\omega) + \frac{A_0}{-i\omega} \tag{29}$$

where $R_0, h_0, A_0 > 0$ are constants that fit a given impedance value $Z(\omega) = Z_R + Z_I i$ at $\omega = \omega_0 > 0$. For example, if $Z_I < 0$ then $R_0 = Z_R, A_0 = 0.1,$ and $h_0 = (A_0/\omega_0 - Z_I)/\omega_0$, and if $Z_I > 0$ then $R_0 = Z_R, h_0 = 0.1,$ and $A_0 = (Z_I + h_0\omega_0)\omega_0$. Taking the inverse Fourier transform and substituting into (9) yields an impedance boundary condition for soft surfaces. Casting into matrix form, the non-zero entries for $\boldsymbol{D}$ and $\boldsymbol{E}$ are, respectively:

$$\{\boldsymbol{D_k}\}_{ij} = \delta_{ij}\rho_0\psi''_{n-k}(t_n) \tag{30}$$

$$\{\boldsymbol{E_k}\}_{ij} = \delta_{ij}[R_0\psi'_{n-k}(t_n) + h_0\psi''_{n-k}(t_n) + A_0\psi_{n-k}(t_n)] \tag{31}$$

where δ_{ij} is a Kronecker delta function and a prime denotes a derivative with respect to time.

As with the *Extended Helmholtz Resonator Model,* the matrices $\boldsymbol{D}$ and $\boldsymbol{E}$ are sparse and represent interactions within the same element or nearby nodes at the same time level t_n. Moreover, the matrices are diagonally dominant and of the form $\boldsymbol{D_k} = d_k\boldsymbol{I}$ and $\boldsymbol{E_k} = e_k\boldsymbol{I}$ where $k = 0,1,\dots,\boldsymbol{K}$

and $\boldsymbol{I}$ is the identity matrix. In particular, the coefficients d_k and e_k simplify to:

$$d_k = \rho_0 \begin{Bmatrix} 2 & k=0 \\ -5 & k=1 \\ 4 & k=2 \\ -1 & k=3 \\ 0 & \text{other} \end{Bmatrix} \tag{32}$$

$$e_k = R_0 \begin{Bmatrix} 11/6 & k=0 \\ -3 & k=1 \\ 3/2 & k=2 \\ -1/3 & k=3 \\ 0 & \text{other} \end{Bmatrix} + h_0 \begin{Bmatrix} 2 & k=0 \\ -5 & k=1 \\ 4 & k=2 \\ -1 & k=3 \\ 0 & \text{other} \end{Bmatrix}$$

$$+2A_0 \begin{Bmatrix} 1 & k=0 \\ 0 & k\neq 0 \end{Bmatrix} \tag{33}$$

Similarly, we may assume the frequency-domain surface admittance model to be:

$$Y(\omega) = \overline{R_0} + \overline{h_0}(-i\omega) + \frac{\overline{A_0}}{-i\omega} \tag{34}$$

Letting the surface admittance be represented in the form for $Y(\omega) = Y_R + Y_I i$, taking the inverse Fourier transform, and substituting into (10) yields an admittance boundary condition for soft surfaces. Casting into matrix form, the non-zero entries for $\boldsymbol{D}$ and $\boldsymbol{E}$ have coefficients d_k and e_k which simplify to:

$$d_k = \rho_0 \overline{R_0} \begin{Bmatrix} 11/6 & k=0 \\ -3 & k=1 \\ 3/2 & k=2 \\ -1/3 & k=3 \\ 0 & \text{other} \end{Bmatrix} + \rho_0 \overline{h_0} \begin{Bmatrix} 2 & k=0 \\ -5 & k=1 \\ 4 & k=2 \\ -1 & k=3 \\ 0 & \text{other} \end{Bmatrix}$$

$$+\rho_0 \overline{A_0} \begin{Bmatrix} 1 & k=0 \\ 0 & k\neq 0 \end{Bmatrix} \tag{35}$$

$$e_k = \begin{Bmatrix} 1 & k=0 \\ 0 & k\neq 0 \end{Bmatrix} \tag{36}$$

Eigenvalue Analysis

As previously mentioned, direct numerical simulation of the TD-BIE without Burton-Miller reformulation is prone to numerical instabilities. It is therefore necessary to study the TD-BIE with Burton-Miller reformulation to ensure stability of the coupled system (19) with liner boundary conditions (9) and (10). To study the stability, we conduct a numerical eigenvalue study of the discretized system of equations [20]. Let us denote Eq. (19) by:

$$\boldsymbol{A_0 w^n = q_0^n - A_1 w^{n-1} - \cdots - A_J w^{n-J}} \tag{37}$$

such that:

$$\boldsymbol{A_K} = \begin{bmatrix} \boldsymbol{B_K} & \boldsymbol{C_K} \\ \boldsymbol{D_K} & \boldsymbol{E_K} \end{bmatrix} \text{ for } k = 0, \dots, K$$

$$\boldsymbol{A_K} = \begin{bmatrix} \boldsymbol{B_K} & \boldsymbol{0} \\ \boldsymbol{0} & \boldsymbol{0} \end{bmatrix} \text{ for } k = K+1, \dots, J \tag{38}$$

$$\boldsymbol{w^n} = \begin{bmatrix} \boldsymbol{u^n} \\ \boldsymbol{v^n} \end{bmatrix} \textbf{ and } \boldsymbol{q_0^n} = \begin{bmatrix} \boldsymbol{q^n} \\ \boldsymbol{0} \end{bmatrix}$$

We look for solutions of the form $\boldsymbol{w^n = \lambda^n e_0}$ to the corresponding homogeneous system given by (37). By substituting $\boldsymbol{w^n = \lambda^n e_0}$ into (37), we obtain a polynomial eigenvalue problem

$$\boldsymbol{\left[A_0 \lambda^J + A_1 \lambda^{J-1} + \cdots + A_{J-1}\lambda^J + A_J\right] e_0 = 0} \tag{39}$$

which can be cast into a generalized eigenvalue problem. The numerical scheme is stable if $|\lambda| \leq 1$ for all eigenvalues. Eigenvalues of the generalized eigenvalue problem can be found via a sparse solver available in MATLAB or Python, or by a matrix power iteration method as detailed in [16].

For the stability study, we consider the scattering of an acoustic point source by a flat plate with dimension $[-0.5,0.5] \times [-0.5,0.5] \times [-0.1,0.1]$. The surface of the flat plate is discretized using $20 \times 20 \times 4$ (1120 surface elements) as illustrated in Figure 3. An acoustic point source is located at $(x, y, z) = (0,0,1)$.

The liner boundary condition is modeled using numerical data in [14]. In [14], eighteen *Extended Helmholtz Resonator Model* models are proposed for varying combinations of $Z(\omega) = A + Bi$ and ν at frequency $\omega_0 = 100$. This numerical data is listed in Table 1. Moreover, two-time steps are considered, namely $\Delta t = 1/24$ and $\Delta t = \pi/1000$.

For the *Extended Helmholtz Resonator Model*, only positive values for ϵ were considered due to the restriction that $\epsilon \geq 0$. Choosing ϵ to be equal to $0.9 \operatorname{arcsinh}(-(A/B)\sin(\omega_0 \nu \Delta t))$ for both the

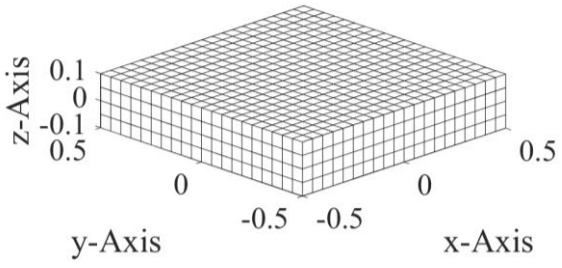

Figure 3: Schematic diagram illustrating the $20 \times 20 \times 4$ *discretization for the flat plate with dimension* $[-0.5,0.5] \times [-0.5,0.5] \times [-0.1,0.1]$ *used for modeling the acoustic scattering of a point source located at* $(x, y, z) = (0,0,1)$.

Table 1: Numerical data for the eighteen different liner models proposed in [14].

Case	$Z(\omega)$	ν
1	$1-3i$	1
2	$1-3i$	5
3	$1-3i$	9
4	$1-2i$	1
5	$1-2i$	5
6	$1-2i$	9
7	$1-i$	1
8	$1-i$	5
9	$1-i$	9
10	$1+i$	19
11	$1+i$	15
12	$1+i$	11
13	$1+2i$	19
14	$1+2i$	15
15	$1+2i$	11
16	$1+3i$	19
17	$1+3i$	15
18	$1+3i$	11

impedance and admittance boundary condition using data in Table 1 limits the study to cases for $\nu = 5$ when $\mathrm{Im}(Z) < 0$ and $\nu = 19{,}15$ when $\mathrm{Im}(Z) > 0$ for $\Delta t = 1/24$ (i.e., Cases 2, 5, 8, 10, 11, 13, 14, 16, and 17); all cases for ν and $Z(\omega)$ yield positive values for ϵ when $\Delta t = \pi/1000$ and are therefore considered for analysis (i.e., Cases 1 through 18 inclusive). Moreover, in each *Extended Helmholtz Resonator Model* analysis, it is assumed that $\omega_0 = 100, \rho_0 = 1,$ and $m = 0$ [14].

For the *Three-Parameter Impedance Model* analysis, the impedance and admittance boundary conditions were also modeled using numerical data in [14]. Unlike with the *Extended Helmholtz Resonator Model*, the parameters R_0, h_0, A_0 for impedance are independent of both Δt and ν. Thus, the impedance parameters are equivalent for $\Delta t = 1/24$ and $\Delta t = \pi/1000$ as well as for $\nu = 1{,}5{,}9$ and $\nu = 19{,}15{,}11$. We therefore consider only six cases for $Z(\omega)$ herein referred to as Cases 1, 4, 7, 10, 13, and 16 when modeling the impedance boundary condition. Similarly, we consider only Cases 1, 4, 7, 10, 13, and 16 when modeling the admittance boundary condition. Note that although the parameters are independent of time-step, the scattering solution differs between $\Delta t = 1/24$ and $\Delta t = \pi/1000$. Hence both scattering solutions will be assessed for their stability in the *Three-Parameter Impedance Model* analysis.

For the stability assessment, we consider two possible scenarios for applying an acoustic liner to the scattering body, the first being that the scattering body is lined on all external surfaces and the second being that the scattering body is lined only on the top-most surface nearest the acoustic point source. We also consider a scattering body with no acoustic liner such that the scattering solution is governed by Eq. (17). An illustration of the fully-lined (soft) body is illustrated in Figure 4. An illustration of the partially-lined (mixed) body is illustrated in Figure 5. An illustration of an un-lined (rigid) body is illustrated in Figure 3, for reference.

All impedance boundary condition (rigid, soft, mixed) results are listed in Table 2. All admittance boundary condition (rigid, soft, mixed) results are listed in Table 3. For both the *Extended Helmholtz Resonator Model* and *Three-Parameter Impedance Model* all eigenvalues are no greater than unity and stability is observed for both the impedance and admittance boundary conditions considering all liner applications: un-lined (rigid), fully-lined (soft), and partially-lined (mixed). These results were expected due to the Burton-Miller type reformulation of the TD-BEM.

Concluding Remarks

A formulation of the acoustic wave scattering of geometric bodies treated with acoustic liners has been proposed. The current work considers using either an impedance or an admittance boundary condition. Each type boundary condition was derived and coupled with a TD-BIE stabilized with a Burton-Miller reformulation. This reformulation eliminates resonant frequencies in the interior domain. An iterative scheme is presented for the solution of the coupled system in the time-domain

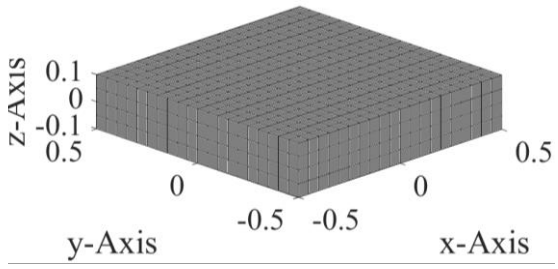

Figure 4: Schematic diagram illustrating a fully-lined body.

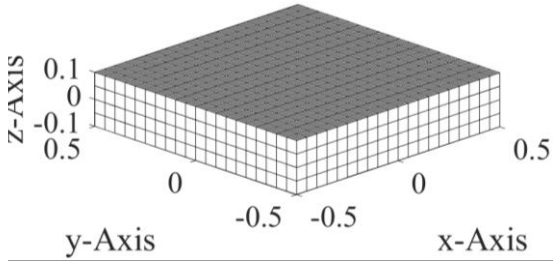

Figure 5: Schematic diagram illustrating a partially-lined body.

Table 2: Maximum eigenvalue calculated for each liner model (Helmholtz, Three-Parameter) and time-step ($1/24$, $\pi/1000$) assuming an impedance boundary condition.

Extended Helmholtz Resonator Model Impedance Boundary Condition				
Δt	Case	Rigid	Soft	Mixed
$\frac{1}{24}$	2	1.000000	1.000000	1.000000
	5	1.000000	1.000000	1.000000
	8	1.000000	1.000000	1.000000
	10	1.000000	0.986059	0.680876
	11	1.000000	1.000000	1.000000
	13	1.000000	0.99106	0.712118
	14	1.000000	0.875391	0.761538
	16	1.000000	0.988567	0.701207
	17	1.000000	0.878414	0.779593
Δt	Case	Rigid	Soft	Mixed
$\frac{\pi}{1000}$	1	1.000000	1.000000	1.000000
	2	1.000000	1.000000	1.000000
	3	1.000000	1.000000	1.000000
	4	1.000000	1.000000	1.000000
	5	1.000000	1.000000	1.000000
	6	1.000000	1.000000	1.000000
	7	1.000000	1.000000	1.000000
	8	1.000000	1.000000	1.000000
	9	1.000000	1.000000	1.000000
	10	1.000000	1.000000	1.000000
	11	1.000000	1.000000	1.000000
	12	1.000000	1.000000	1.000000
	13	1.000000	1.000000	1.000000
	14	1.000000	1.000000	1.000000
	15	1.000000	1.000000	1.000000
	16	1.000000	1.000000	1.000000
	17	1.000000	1.000000	1.000000
	18	1.000000	1.000000	1.000000
Three-Parameter Impedance Model Impedance Boundary Condition				
Δt	Case	Rigid	Soft	Mixed
$\frac{1}{24}$	1	1.000000	1.000000	1.000000
	4	1.000000	1.000000	1.000000
	7	1.000000	1.000000	1.000000
	10	1.000000	1.000000	1.000000
	13	1.000000	1.000000	1.000000
	16	1.000000	1.000000	1.000000
Δt	Case	Rigid	Soft	Mixed
$\frac{\pi}{1000}$	1	1.000000	1.000000	1.000000
	4	1.000000	1.000000	1.000000
	7	1.000000	1.000000	1.000000
	10	1.000000	1.000000	1.000000
	13	1.000000	1.000000	1.000000
	16	1.000000	1.000000	1.000000

Table 3: Maximum eigenvalue calculated for each liner model (Helmholtz, Three-Parameter) and time-step ($1/24$, $pi/1000$) assuming an admittance boundary condition.

Extended Helmholtz Resonator Model Admittance Boundary Condition				
Δt	Case	Rigid	Soft	Mixed
$\frac{1}{24}$	2	1.000000	0.999884	1.000000
	5	1.000000	0.999933	1.000000
	8	1.000000	0.999991	1.000000
	10	1.000000	1.000000	1.000000
	11	1.000000	1.000000	1.000000
	13	1.000000	1.000000	1.000000
	14	1.000000	1.000000	1.000000
	16	1.000000	1.000000	1.000000
	17	1.000000	1.000000	1.000000
Δt	Case	Rigid	Soft	Mixed
$\frac{\pi}{1000}$	1	1.000000	1.000000	1.000000
	2	1.000000	1.000000	1.000000
	3	1.000000	0.943965	1.000000
	4	1.000000	1.000000	1.000000
	5	1.000000	1.000000	1.000000
	6	1.000000	0.938683	1.000000
	7	1.000000	1.000000	1.000000
	8	1.000000	1.000000	1.000000
	9	1.000000	0.999999	1.000000
	10	1.000000	1.000000	1.000000
	11	1.000000	1.000000	1.000000
	12	1.000000	0.999998	1.000000
	13	1.000000	1.000000	1.000000
	14	1.000000	1.000000	1.000000
	15	1.000000	0.999993	1.000000
	16	1.000000	1.000000	1.000000
	17	1.000000	1.000000	1.000000
	18	1.000000	0.999999	1.000000
Three-Parameter Impedance Model Admittance Boundary Condition				
Δt	Case	Rigid	Soft	Mixed
$\frac{1}{24}$	1	1.000000	0.998003	1.000000
	4	1.000000	0.998003	1.000000
	7	1.000000	0.998002	1.000000
	10	1.000000	0.999928	1.000000
	13	1.000000	0.999928	1.000000
	16	1.000000	0.999928	1.000000
Δt	Case	Rigid	Soft	Mixed
$\frac{\pi}{1000}$	1	1.000000	0.199984	1.000000
	4	1.000000	0.223336	1.000000
	7	1.000000	0.200312	1.000000
	10	1.000000	0.999995	1.000000
	13	1.000000	0.999995	1.000000
	16	1.000000	0.999995	1.000000

which uses spatial and temporal basis functions and allows for acoustic scattering problems to be modeled with geometries consisting of both rigid and soft surfaces. Three different liner applications were considered: un-lined, fully-lined, and partially-lined. Moreover, two models were considered when simulating the acoustic liner: an *Extended Helmholtz Resonator Model* [14] and a *Three-Parameter Impedance Model* [17]. In each model, the acoustic liner impedance is specified at a single

frequency. Eigenvalue analysis was presented for the scattering solution by a flat plate discretized with 1120 surface elements. The eigenvalue analysis demonstrated stable solutions for both the impedance and admittance boundary conditions considering all liner applications: un-lined (rigid), fully-lined (soft), and partially-lined (mixed). Future work will include studying a broadband acoustic liner model to allow for the investigation of multiple frequencies simultaneously.

Acknowledgments

F. Q. Hu and M. E. Rodio are supported by a NASA Cooperative Agreement, NNX11AI63A. This work used the computational resources at the Old Dominion University ITS Turing cluster and the Extreme Science and Engineering Discovery Environment (XSEDE), which is supported by National Science Foundation grant number OCI-1053575.

Citations

[1] F. Q. Hu, "An Efficient Solution of Time Domain Boundary Integral Equations for Acoustic Scattering and Its Acceleration by Graphics Processing Units," in *American Institute of Aeronautics*, Washington, DC, 2013.

[2] F. Q. Hu, "Further Development of a Time Domain Boundary Integral Equation Method for Aeroacoustic Scattering Computations," in *20th AIAA/CEAS Aeroacoustics Conference*, Washington, DC, 2014.

[3] F. Q. Hu, M. E. Pizzo and D. M. Nark, "On the Assessment of Acoustic Scattering and Shielding by Time Domain Boundary Integral Equation Solutions," in *22nd AIAA/CEAS Aeroacoustics Conference*, Washington, DC, 2016.

[4] F. Q. Hu, M. E. Pizzo and D. M. Nark, "A New Formulation of Time Domain Boundary Integral Equation for Acoustic Wave Scattering in the Presence of a Uniform Mean Flow," in *23rd AIAA/CEAS Aeroacoustics Conference*, Washington, DC, 2017.

[5] D. J. Chappell, P. J. Harris, D. Henwood and R. and Chakrabarti, "A Stable Boundary Element Method for Modeling Transient Acoustic Radiation," *Journal of the Acoustical Society of America,* vol. 120, no. 1, pp. 74-80, 2006.

[6] A. A. Ergin, B. Shankar and E. and Michielssen, "Analysis of TransientWave Scattering from Rigid Bodies Using a Burton-Miller Approach," *Journal of the Acoustical Society of America,* vol. 106, no. 5, p. 2396–2404, 1999.

[7] A. D. Jones and F. Q. Hu, "A Three-Dimensional Time-Domain Boundary Element Method for the Computation of Exact Green's Functions in Acoustic Analogy," in *13th AIAA/CEAS Aeroacoustics Conference*, Washington, DC, 2007.

[8] S. Marburg, "The Burton and Miller Method: Unlocking Another Mystery of Its Coupling Parameter," *Journal of Computational Acoustics,* vol. 23, no. 1550016, 2015.

[9] S. Marburg and S. Schneider, "Influence of Element Types on Numeric Error for Acoustic Boundary Elements," *Journal of Computational Acoustics,* vol. 11, no. 3, pp. 363-386, 2001.

[10] R. J. Astley and G. J. Macaulay, "Three-Dimensional Wave-Envelope Elements of Variable Order for Acoustic Radiation and Scattering. Part I. Formulation in the Frequency Domain," *Journal of the Acoustical Society of America,,* vol. 103, no. 1, pp. 49-63, 1998.

[11] A. Kierkegaard, S. Boij and G. Efraimsson, "A Frequency Domain Linearized Navier-Stokes Equations Approach to Acoustic Propogation in Flow Ducts with Sharp Edges," *Journal of the Acoustical Society of America,* vol. 142, no. 4, pp. 710-719, 2010.

[12] A. Iob, R. Arina and C. Schipani, "Frequency-Domain Linearized Euler Model for Turbomachinery Noise Radiation Through Engine Exhaust," *American Institute of Aeronautics and Astronautics Journal,* vol. 48, no. 4, pp. 848-858, 2010.

[13] C. K. W. Tam and L. Auriault, "Time-Domain Impedance Boundary Conditions for Computational Aeroacoustics," *American Institute of Aeronautics and Astronautics Journal,* vol. 34, no. 5, pp. 917-923, 1996.

[14] S. W. Rienstra, "Impedance Models in Time Domain Including the Extended Helmholtz Resonator Model," in *12th AIAA/CEAS Aeroacoustics Conference*, Washington, DC, 2006].

[15] A. M. N. Spillere, A. A. Medeiros and J. S. Cordiolo, "An Improved Impedance Education Technique Based on Impedance Models and the Mode Matching Method,"

Applied Acoustics, vol. 129, no. 2018, pp. 322-334, 2017.

[16] M. E. Pizzo, F. Q. Hu and D. M. Nark, "Simulation of Sound Absorption by Scattering Bodies Treated with Acoustic Liners Using a Time-Domain Boundary Element Method," in *24th AIAA/CEAS Aeroacoustics Conference*, Washington, DC, 2018.

[17] C. K. W. Tam, Computational Aeroacoutics: A Wave Number Approach, 1 ed., New York: Cambridge University Press, 2012.

[18] P. M. Morse and K. U. Ingard, Theoretical Acoustics, 1 ed., Princeton: Princeton University Press, 1986.

[19] F. Q. Hu, P. M. E and N. D. M, "On a Time Domain Boundary Integral Equation Formulation for Acoustic Scattering by Rigid Bodies in Uniform Mean Flow," *Journal of the Acoustical Society of America,* vol. 142, no. 6, pp. 3624-3636, 2017.

[20] S. J. Dodson, S. P. Walker and M. J. Bluck, "Impicitness and Stability of Time Domain Integral Equation Scattering Analysis," *Applied Computational Electromagnetics Society Journal,* vol. 13, pp. 291-301, 1998.